

Nanoscale

Accepted Manuscript



This is an *Accepted Manuscript*, which has been through the Royal Society of Chemistry peer review process and has been accepted for publication.

Accepted Manuscripts are published online shortly after acceptance, before technical editing, formatting and proof reading. Using this free service, authors can make their results available to the community, in citable form, before we publish the edited article. We will replace this *Accepted Manuscript* with the edited and formatted *Advance Article* as soon as it is available.

You can find more information about *Accepted Manuscripts* in the [Information for Authors](#).

Please note that technical editing may introduce minor changes to the text and/or graphics, which may alter content. The journal's standard [Terms & Conditions](#) and the [Ethical guidelines](#) still apply. In no event shall the Royal Society of Chemistry be held responsible for any errors or omissions in this *Accepted Manuscript* or any consequences arising from the use of any information it contains.

Temperature Dependence of the Radiative Lifetimes in Ge and Si Nanocrystals[†]

Nancy C. Forero-Martinez^a, Ha-Linh Thi Le^a, Ning Ning^a, Holger Vach^a and Hans-Christian Weissker^{*b,c}

The effect of finite temperature on the optical properties of nanostructures has been a longstanding problem for their theoretical description and their omission presented serious limits on the validity of calculated spectra and radiative lifetimes. Most *ab initio* calculations have been carried out neglecting temperature effects altogether, although progress has been made recently. In the present work, the temperature dependence of the intrinsic radiative lifetimes of excited electron-hole pairs in Ge and Si nanocrystals due to classical temperature effects is calculated using *ab initio* molecular dynamics. Fully hydrogen-saturated Ge and Si nanocrystals without surface reconstructions show opposite behavior: the very short lifetimes in Ge increase with temperature, while the much longer ones in Si decrease. However, the temperature effect is found to be strongly dependent on the surface structure: surface reconstructions cause partial localization of the wave functions and override the difference between Si and Ge. As a consequence, the temperature dependence in reconstructed nanocrystals is strongly attenuated compared to the fully saturated nanocrystals. Our calculations are an important step towards predictive modeling of the optical properties of nanostructures.

Temperature effects have been neglected in practically all the calculations of the optical properties of semiconductor nanocrystals, which have been carried out mostly using density-functional theory (DFT) and time-dependent DFT (TDDFT) at zero temperature, i.e., using fixed atomic positions. Nonetheless, the effects of temperature cannot be entirely disregarded, as it is known experimentally^{1,2} and theoretically for bulk materials³ and nanostructures.^{4–10} In metal clusters even the basic character of the absorption spectra and the amount of spectroscopically accessible information on the

quantum nature of the clusters can be entirely obscured by temperature effects and become clear only at low temperature.¹¹ In addition, the importance of the nuclear zero-point motion has been demonstrated recently.^{9,12,13} In particular, Patrick *et al.* have demonstrated that the static geometries of nano-diamondoids lead to entirely inadequate simulated spectra, whereas the inclusion of the quantum nuclear motion leads to good agreement with experiment. In addition, likewise for diamondoids, vibrationally resolved spectra have been calculated in good agreement with experiment based on the Franck-Condon principle.¹⁴ For hydrogen-saturated Si NCs, temperature induces a size-dependent, non-negligible decrease^{6,8} of the HOMO-LUMO gaps, which is likewise demonstrated by many experiments that show a shift of PL peak energies with changing temperature.^{15,16} This raises the practically relevant question as to how the finite temperature influences the radiative lifetimes and, hence, the luminescence intensity, for which much less material is available for comparison.

Silicon and germanium nanocrystals (NCs) have been used in many applications, ranging from optoelectronics and light emission to photovoltaics and the use as biomarkers. As bulk materials, the two elements are indirect semiconductors. The basic idea of their use as optically active nanostructures relies on breaking the **k** selection when translational symmetry is no longer present. The gradual development of **k** selection with increasing size has been explicitly demonstrated by Kocovski *et al.*¹⁷ For Si, the indirect nature of the bulk band gap carries over to Si nanostructures, resulting in weak HOMO-LUMO transitions (transitions between the highest occupied molecular orbital and the lowest unoccupied molecular orbital) and, consequently, long radiative lifetimes (LTs)^{17–21} which are, however, strongly size-dependent.^{19,22} By contrast, a number of different geometries of Ge nanostructures have been predicted to show strong HOMO-LUMO transitions,^{20,21,23–25} reminiscent of direct semiconductors. Moreover, strained Ge has been used to obtain optical gain and lasing.^{26,27} In addition, alloying with Ge reduces the radiative lifetimes of Si nanocrystals.^{28–30} However, little luminescence from Ge nanostructures has been found that could clearly be attributed to the recombination of confined electron-hole pairs. Most luminescence found has been related to defect or interface states^{31,32} just as in the case of oxidized Si nanostructures.^{33–35} By contrast, laser pyrolysis³⁶ and plasma-

[†] Electronic Supplementary Information (ESI) available: To complement the averaged quantities discussed in the paper, we show individual transition probabilities for both the Kohn-Sham transitions and the TDDFT transitions for the ground-state geometry and for snapshots from the trajectories at finite temperature. Moreover, we show the HOMO and LUMO states for two reconstructed structures to complement the figures in the article.

^a LPICM, Ecole Polytechnique, CNRS, 91128 Palaiseau, France.

^b Aix Marseille University, CNRS, CINaM UMR 7325, 13288, Marseille, France.

^c European Theoretical Spectroscopy Facility (ETSF).

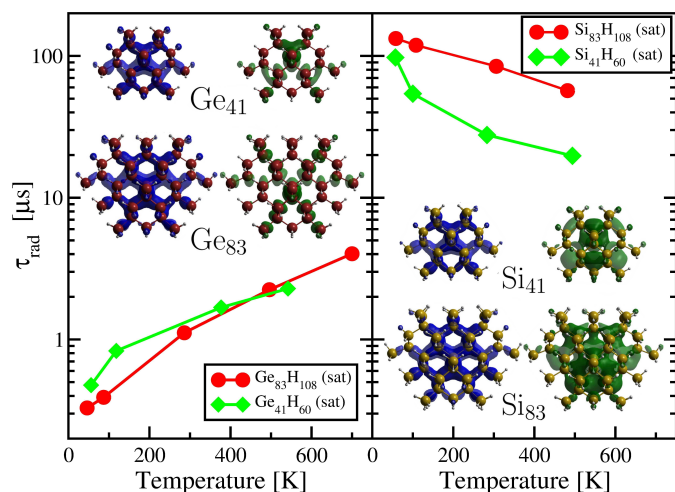


Fig. 1 The lifetimes of two sizes of the fully saturated NCs without reconstructions on the surfaces. In the low-temperature limit, lifetimes are much shorter in Ge than in Si NCs. Increasing temperature leads to opposite changes for Ge and Si. We also show the HOMO (blue) and the LUMO (green) states ($|\psi|^2$ at 10% of the maximum value) of the respective NCs at $T = 0$. The HOMO states are almost the same in the Ge and the Si NCs, while the LUMO states are clearly different. n_{eff} is set to 1.

enhanced chemical vapor deposition (PECVD) under certain conditions³⁷ produce clean, hydrogenated nanocrystals where the intrinsic properties are expected to determine the optical properties. A previous work has demonstrated that compression increases the radiative lifetimes in Ge nanocrystals drastically.³⁸ In addition, surface reconstructions change the radiative lifetimes³⁸ which is due to strong changes in the electronic structure.^{38–40} The role of temperature effects on the radiative lifetimes, however, has not been fully elucidated to date. Often in the past, the Boltzmann distribution of the thermalized electron-hole pairs has been taken into account while the lattice vibrations were neglected^{18,20,22,41}.

In the present study, we show that classical finite temperature effects increase the radiative lifetimes in fully saturated Ge nanocrystals that show strong HOMO-LUMO transitions and efficient luminescence in zero-temperature calculations, whereas equivalent Si nanocrystals show the opposite behavior. In a second step, we show that the surface structure plays a very important role: surface reconstructions are found to override the difference of the temperature dependence between Ge and Si nanocrystals.

We study two different types of nanocrystals. Fully H-saturated NCs are constructed starting from one Ge or Si atom and adding nearest neighbors shell by shell, with bulk-like coordination. Subsequently, all dangling bonds are saturated by hydrogen atoms. The resulting NCs are Ge_5H_{17} , $\text{Ge}_{41}\text{H}_{60}$,

$\text{Ge}_{83}\text{H}_{108}$, $\text{Ge}_{147}\text{H}_{148}$ and their Si counterparts. These completely saturated NCs, which have also been called “bulk-like” in previous work, are of T_d symmetry and have been studied extensively in the past.^{19,20,30,42} Their HOMO and LUMO wave functions are spread out over the entire NC,⁴² the size-dependence of their HOMO-LUMO gaps clearly follows the quantum confinement model,^{20,43} and the character of the lowest transitions reflects the nature of the bulk material:^{19,20,42} the Ge NCs show strong HOMO-LUMO transitions, while for Si the transitions around the gap are weak.^{20,29}

Second, as this type of perfect surface structure cannot be expected to be representative for all NCs in realistic experimental situations, we also study “reconstructed” NCs: a spherical structure is cut from the bulk using a given radius and centered at an atom. One-fold coordinated atoms are removed and two-fold coordinated atoms are bonded to form 2×1 dimers. The rest of the dangling bonds is saturated by hydrogen atoms. The resulting structures $\text{Ge}_{29}\text{H}_{24}$, $\text{Ge}_{53}\text{H}_{36}$, $\text{Ge}_{98}\text{H}_{56}$ and their Si counterparts turn out to be rather stable. The Si NCs have been heated up to 1500 K in classical molecular dynamics calculations without breaking. However, the gaps in these structures do not fit the monotonous $1/d$ decrease with increasing size of the confinement model, although a general decrease of the gaps with increasing size is also found.^{39,40}

To consider temperature effects, explicit calculation of lattice-vibrations of clusters and nanocrystals using Born-Oppenheimer molecular dynamics with a subsequent averaging to obtain the desired quantities has been employed in a number of studies considering small Si clusters,⁵ sodium clusters,⁴ and hydrogenated Si nanocrystals.⁸ In the present study, we use this approach, which is justified by the fact that the radiative lifetimes are longer than the vibrational periods of the thermal vibrations. We calculate the vibrations using *ab initio* molecular dynamics as implemented in the VASP code⁴⁴ using density-functional theory (DFT) in the local-density approximation (LDA) and with the projector-augmented wave method.⁴⁵ The structures are heated and equilibrated at a given temperature followed by *ab initio* MD calculations in the microcanonical ensemble (NVE). These calculations correspond to free NCs in vacuum, as for instance those formed in the gas phase of PECVD before deposition on a substrate.³⁷ Beyond distortions, the structures remain unchanged, i.e., no bonds are broken or formed. Time steps ranging from 0.1 fs to 0.75 fs are used depending on the NC size. Production trajectories last 5 ps. The temperature of the nanoclusters is obtained as average over the whole trajectory. The rotational part of the kinetic energy is subtracted.⁴⁶ Zero-point vibrations are neglected. The radiative lifetimes τ are calculated following Ref. 18 assuming thermalized electron-hole pairs. The thermally averaged transition probability^{18,41}

$$\frac{1}{\tau} = n_{\text{eff}} \frac{4e^2}{\hbar^2 mc^3} \frac{\sum_{cv} f_{cv} \epsilon_{cv}^2 e^{-\epsilon_{cv}/kT}}{\sum_{cv} e^{-\epsilon_{cv}/kT}}, \quad (1)$$

where f_{cv} are the oscillator strengths (cf. Supp. Mat. for their definition) and ϵ_{cv} the transition energies, is calculated using the transition matrix elements calculated for the Kohn-Sham system in the same way as it has been done before for calculations at zero temperature.^{19,20,22,29} n_{eff} is the refractive index of the surrounding matrix which we assume to be 1 in the present calculations. The temperature-dependent lifetimes are obtained by sampling 100 snapshots from the respective trajectories. To double-check the statistical validity of our sampling, a comparison with longer trajectories and higher numbers of snapshots is shown in the Supplementary Material, Fig. S6. Moreover, as a further consistency check for the calculations, we show the temperature dependence of the HOMO-LUMO gap in the Supplementary Material, Fig. S7; our results are consistent with previous work of other groups.⁸

In the present calculations, spin-orbit coupling is neglected. While this is certainly well justified for Si, this requires discussion for Ge. In Ref. 38, some of us have shown that in the 41-atom fully H-saturated Ge nanocrystal, the strong lowest transition is split by the spin-orbit interaction, which leads to an increase of the lifetimes, estimated to be at most by a factor of 5. This increase is not as large as to interfere with the fundamental difference between Ge and Si NCs. Consequently, it is not expected to change the general findings of the present study of the effect of finite temperature.

(1) Fully saturated Ge and Si nanocrystals. The radiative lifetimes are shown in Fig. 1. In the low-temperature limit, the fully saturated NCs show the well-known strong difference between Ge and Si, with lifetimes being shorter by two to three orders of magnitude in Ge, as it has been reported before.^{20,38,42} The main finding of the present work is that the temperature dependence is opposite between Ge and Si: in Ge, the lifetimes increase monotonously, by about one order of magnitude for a temperature of about 500 K, while a decrease of similar magnitude is seen for the Si nanocrystals.

The explanation of this temperature dependence of the radiative lifetimes and, therefore, of the predicted luminescence intensities, hinges on the instantaneous distortions. Due to the exponential factor in Eq. (1), the lowest transitions and, in particular, the HOMO-LUMO transitions determine the radiative lifetimes decisively. At zero temperature, our NCs are high-symmetry structures of T_d symmetry and the HOMO is threefold degenerate for both Si and Ge (times two for spin). This corresponds to the valence-band maximum at Γ in the bulk. Consequently, the HOMO state is very similar for Ge and Si NCs of equal geometry, as can be seen in Fig. 1. The lowest transition in the Ge NCs is a very strong, degenerate HOMO-LUMO transition which reflects the strong contribu-

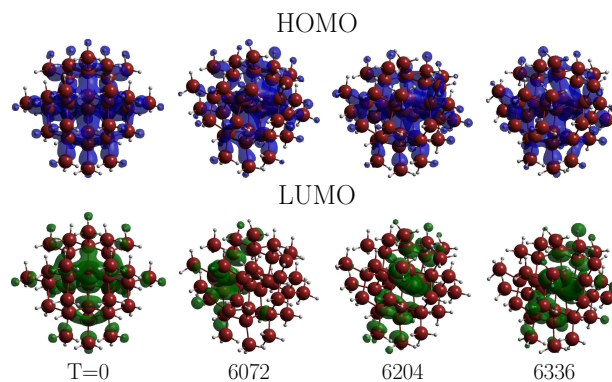


Fig. 2 HOMO and LUMO states of the fully saturated $\text{Ge}_{41}\text{H}_{60}$ NC ($|\psi|^2$ at 10% of maximum value) at $T=0$ and three snapshots out of the trajectory at 118 K, the numbers indicating the ionic step. We show the sum of the HOMO states that are three-fold degenerate at $T=0$, but only approximately degenerate at 118 K. The LUMO is not degenerate and changes drastically between the different snapshots along the trajectory due to the instantaneous distortions.

tion of the Γ - Γ transition that in the bulk is only slightly higher in energy than the minimum gap Γ -L.³⁸ This has been demonstrated in Ref. 38 where in addition to the heuristic argument referring to the strong lowest transitions, the comparison of the pressure dependence of the NC HOMO-LUMO gaps with the pressure dependence of the different bulk gaps (Γ - Γ , Γ -X, Γ -L) demonstrated the role of the Γ - Γ contribution in the Ge NCs. By contrast, the oscillator strength of the lowest transitions in Si BCs is rather small, reflecting the strongly indirect behavior of bulk Si that carries over to the NCs. Both the degeneracy and the high (low) transition probabilities in Ge (Si) are thus connected with the symmetry of the wavefunctions.

Upon heating, the NCs start to vibrate and distort (without breaking or forming bonds). The effect of the instantaneous distortions can be seen in Fig. 2 where we compare, for the fully saturated $\text{Ge}_{41}\text{H}_{60}$, the wave functions at 0 K and of three different snapshots out of the trajectory at 118 K. At 0 K, only the sum of the three degenerate HOMO states has a clear physical meaning. For better comparability, we show the average of the three lowest states also for the snapshots, although there the degeneracy is lifted, with energy differences of 0.05 to 0.10 eV between the states. Clearly, this averaged “HOMO” does not show strong modifications over the course of the vibration. By contrast, the LUMO state, non-degenerate for $T=0$, changes very strongly due to the instantaneous distortions, thus producing the change in the transition matrix elements and, therefore, of the radiative lifetimes.

The symmetry aspect and, therefore, the instantaneous distortions, are of paramount importance. In Ge at $T=0$, the very strong Γ - Γ -like transitions are due to the largely undisturbed Γ - Γ character that carried over from the bulk. The instantana-

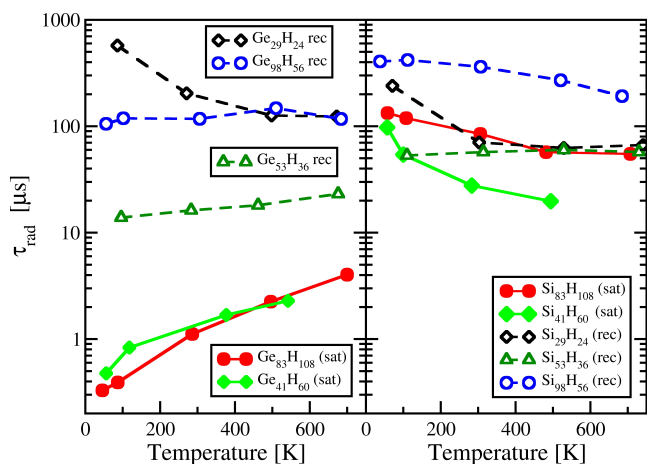


Fig. 3 The effect of the surface reconstruction. Radiative lifetimes of the “reconstructed” (rec) nanocrystals are shown with hollow symbols and dashed lines and compared to their fully saturated (sat) counterparts already shown in Fig. 1 and which are given by full symbols and solid lines for direct comparison. The temperature dependence of the LTs is less strong in the reconstructed NCs and does not follow a clear common trend, unlike in the case of the fully saturated NCs. n_{eff} is set to 1.

neous distortions at finite temperature perturb the symmetry of the system. Consequently, the exceptionally strong Γ - Γ -like transitions lose part of their strength. This is the reason why the radiative lifetimes in Ge NCs *increase* with increasing temperature. In Si, by contrast, the lowest transitions are approximately *forbidden*, i.e., in the NC, very weak. This is likewise due to the symmetry. As the symmetry is perturbed upon heating, the “forbiddenness” is mitigated, the transitions become stronger, and the radiative lifetimes longer.

This is illustrated in the Supplementary Material, Figs. S1 & S2, for the case of the fully H-saturated $\text{Ge}_{83}\text{H}_{108}$ and $\text{Si}_{83}\text{H}_{108}$ at 100 K. At $T = 0$, i.e., for static lattice, the oscillator strength of the HOMO-LUMO transition is about 400 times larger in $\text{Ge}_{83}\text{H}_{108}$ than in $\text{Si}_{83}\text{H}_{108}$ (note the logarithmic y axis). The following group of transitions is forbidden. For the finite-temperature snapshots, the symmetry is broken and two things change: (i) the degeneracies are lifted and (ii) the symmetry-related selection rules are softened. The very strong degenerate HOMO-LUMO transition of $\text{Ge}_{83}\text{H}_{108}$ is split and becomes slightly weaker (the $T = 0$ HOMO-LUMO transition is the highest value of all). This decrease causes an increase of the LTs. Likewise, the fact that now only one transition is lowest and all the others that were degenerate with it differ in energy, means that the thermal average with the Boltzmann factor (cf. eq. (1)) leads to a further increase of the lifetimes.

In the case of Si_{83} , the lowest transition is rather weak

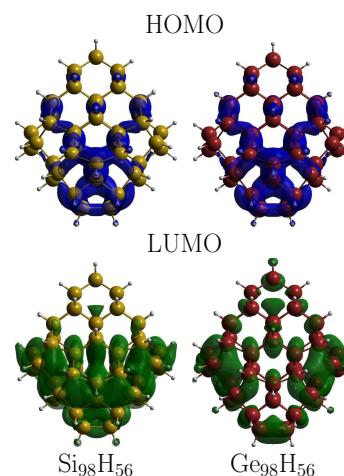


Fig. 4 Ground-state HOMO and LUMO states of the “reconstructed” $\text{Ge}_{98}\text{H}_{56}$ and $\text{Si}_{98}\text{H}_{56}$, showing the strong localization of both HOMO and LUMO states on a part of the surface. The LUMO states show a strong similarity between Si and Ge, unlike for the fully saturated nanocrystals shown in Fig. 1. This similarity leads to the similar values and T dependence of the LTs.

(but not exactly zero) for the $T = 0$ rigid-geometry high-symmetry structure, and there is a rather large number of likewise weak transitions close to it.¹⁹ Kocevski *et al.* have explicitly shown how \mathbf{k} selection develops gradually with increasing size, which of course reflects the symmetry of the system. The relatively weak transitions are degenerate in energy. Upon heating, the symmetries are broken in the vibrating structure and stronger transitions become possible. This is seen by the fact that, unlike in Ge_{83} , the lowest transition in Si_{83} is not the strongest compared to transitions at neighboring energies in the heated NC. Thus the change leads to the increase of the averaged transition rate and, therefore, the decrease of the LTs. The difference of the temperature behavior in Ge and Si is, therefore, closely related to the qualitative difference at zero temperature.

Verification using TDDFT: In order to study this effect beyond the averages based on eq. 1 with its use of Kohn-Sham energies and transition probabilities, we inspect the individual transitions of the same snapshots from the 100 K trajectory of the fully saturated $\text{Ge}_{83}\text{H}_{108}$ and $\text{Si}_{83}\text{H}_{108}$. Knowing the limitations of the Kohn-Sham transition energies and probabilities shown in Figs. S1 and S2 of the Supplementary Material, we calculated the same quantities within time-dependent density-functional theory in the Casida formulation⁴⁷ using the octopus code⁴⁸ (Figs. S2 and S4 of the Supplementary Material). While the numbers are somewhat different, exactly the same conclusions arise for the two different approximations. Future work should produce a systematic comparison

of the lifetimes obtained for the Kohn-Sham-based and the TDDFT-based quantities, depending on both type (fully saturated vs. reconstructed) and material (Si vs. Ge), as well as on the size of the nanocrystals.

(2) Influence of surface reconstructions. The radiative lifetimes for the “reconstructed” Ge and Si NCs are shown in Fig. 3. It has been shown in calculations for static geometries, i.e., at $T = 0$ and neglecting zero-point motion effects, that such reconstructions can decisively change the electronic and optical properties.^{38–40} The surface reconstructions also change the temperature dependence of the radiative lifetimes strongly. The strong difference between Ge and Si found at $T = 0$ for the fully saturated NCs has almost disappeared. For the cases we studied, the radiative lifetimes at low temperature are of the same order of magnitude for structurally equivalent reconstructed Ge and Si NCs, and the temperature dependence is weak and different for different structures. To understand the difference, we investigate again the HOMO and the LUMO wavefunctions. They are shown in Fig. 4 for the “reconstructed” $\text{Ge}_{98}\text{H}_{56}$ and $\text{Si}_{98}\text{H}_{56}$, and in the Supplementary Material for $\text{Ge}_{29}\text{H}_{24}$ and $\text{Ge}_{53}\text{H}_{36}$ and their Si counterparts. Both HOMO and LUMO are not anymore spread out over the whole NC volume but localized on (a part of) the surface. The HOMO states are again identical for equal Ge and Si structures. However, now also the LUMO states show similar localization. This localization evidently overrides the strong difference between Ge and Si found for the fully saturated NCs that reflected the characteristics of the bulk materials. In particular, the LUMO states of $\text{Ge}_{29}\text{H}_{24}$ and $\text{Si}_{29}\text{H}_{24}$ are very similar (see Supplementary Material) which in turn explains the very similar temperature dependence of the lifetimes.

This shows that the detailed surface structure is decisive not only for the absolute value of the radiative lifetimes but also for their temperature dependence. This, in turn, makes comparison with experiment rather difficult, in particular because the reconstructed Ge and Si NCs do not show a coherent trend, as it is clear from Fig. 3. Measured lifetimes are due to both radiative and non-radiative processes. Also the non-radiative processes are strongly energy dependent (see, for instance, measurement and discussion in Hartel *et al.*²) Changes in both the absolute intensities or in explicitly measured lifetimes are, therefore, only partially due to changes in the radiative lifetimes. In addition, it has been shown that the temperature dependence of the PL intensity is strongly dependent on the excitation power density.²

On the other hand, the change of PL peak energies and optical gaps is much more easily comparable. In general, the peak energies decrease with temperature, as do the gaps. This is well known for bulk materials¹ and has likewise been reported

for nanocrystals, see e.g., Van Sickle *et al.*,¹⁵ Derr *et al.*,⁴⁹ and Yu *et al.*,¹⁶ and for InP/ZnS Core-shell QDs.⁵⁰ The change of the gaps has been calculated by Franceschetti⁸ who demonstrated likewise the dependence on the NC size of the temperature effects. Our results are consistent with his, as shown in the Supp. Mat., Fig. S7.

For the lifetimes in Si NCs, a decrease with increasing temperature has been reported, e.g., by Van Sickle *et al.*¹⁵ and by Yu *et al.*¹⁶ This is in line with our results for the fully H-saturated Si nanocrystals. However, care should be taken not to jump to conclusions. Part of the temperature dependence is due to the different temperature dependencies of radiative and non-radiative processes. Hartel *et al.* divide the intensity characteristics into a low-temperature region dominated by radiative decay, and a high-temperature region dominated by non-radiative processes.² Finally, according to the model of Calcott,^{51,52} a temperature dependence is likewise introduced by the exchange-splitting between singlet and triplet exciton. Both these effects are not represented by our calculations.

The part of the temperature dependence that we describe, i.e., the classical effect due to lattice vibrations, is very important. Nonetheless, the other effects, notably the temperature dependence of non-radiative decay channels and of defect luminescence,⁵³ will have to be studied as well. The combination of the different effects will then present the full temperature dependence. Still, in particular the surface structure will have to be carefully controlled so as to make precise comparisons possible.

In conclusion, we have shown that the temperature dependence of the intrinsic radiative lifetimes in semiconductor nanocrystals is strong. In the fully saturated Ge and Si nanocrystals, the temperature dependence due to classical temperature effects is opposite, with a strong monotonous increase for Ge, and a strong decrease for Si. This behavior is due to the change of the individual transition probabilities: the instantaneous vibrational distortion weakens the strong lowest transitions in Ge, where the change is traced back to a strong change of the LUMO, and increases the transition probabilities of the very weak transitions in Si at $T = 0$.

In a second step, we have shown that surface reconstructions cause partial localization of the wavefunctions, overriding the strong difference between Ge and Si, and reducing the temperature dependence compared to the fully saturated nanocrystals.

To the best of our knowledge, these are the first calculations of classical temperature effects due to thermal vibrations on the intrinsic radiative lifetimes in semiconductor nanocrystals. They provide an important step towards truly predictive simulation because they go beyond the restriction to zero temperature which imposed serious limits on the validity of the large majority of previous optical calculations. Our

work is hoped to provide a basis for future comparison with experiment by identifying, quantifying, and explaining the mechanisms that produce the temperature dependence of *intrinsic* luminescence in semiconductor nanocrystals. Naturally, experiment measures a combination of different decay mechanisms including nonradiative recombination due to defects, defect luminescence, interface effects, etc. The theoretical description of each of these will be a research topic on its own, and it is the elucidation of the temperature dependence of each of these contributions one by one which will finally lead to a clear understanding of their combination in a given measurement and provide the means to quantitatively describe and predict luminescence. We would be glad if our work motivated the respective measurements in order to obtain a test of our methodology but, in particular, in order to obtain a detailed understanding of the combination of intrinsic and extrinsic radiative as well as nonradiative decay. The results will be important not only for semiconductor NCs but also, e.g., for luminescent metal clusters.

We gratefully acknowledge discussions with Friedhelm Bechstedt and Lucia Reining. HCW gratefully acknowledges help from Grit Kunert for the statistical analysis. We acknowledge financial support from the EADS Foundation under the project SiNCopes (Ref. 096-AO09-1006). Computer time was granted by the IDRIS, Projects No. GENCI 544 and No. 0910642.

References

- M. Cardona, *Solid State Communications*, 2005, **133**, 3 – 18.
- A. M. Hartel, S. Gutsch, D. Hiller and M. Zacharias, *Phys. Rev. B*, 2012, **85**, 165306.
- A. Marini, *Phys. Rev. Lett.*, 2008, **101**, 106405.
- M. L. del Puerto, M. L. Tiago and J. R. Chelikowsky, *The Journal of Chemical Physics*, 2007, **127**, 144311.
- N. Binggeli and J. R. Chelikowsky, *Phys. Rev. Lett.*, 1995, **75**, 493–496.
- D. Prendergast, J. C. Grossman, A. J. Williamson, J.-L. Fattebert and G. Galli, *Journal of the American Chemical Society*, 2004, **126**, 13827–13837.
- N. A. Murugan, I. Dasgupta, A. Chakraborty, N. Ganguli, J. Kongsted and H. gren, *The Journal of Physical Chemistry C*, 2012, **116**, 26618–26624.
- A. Franceschetti, *Phys. Rev. B*, 2007, **76**, 161301.
- E. Cannuccia and A. Marini, *Phys. Rev. Lett.*, 2011, **107**, 255501.
- S. Cronin, Y. Yin, A. Walsh, R. Capaz, A. Stolyarov, P. Tangney, M. Cohen, S. Louie, A. Swan, M. Ünli, B. Goldberg and M. Tinkham, *Phys. Rev. Lett.*, 2006, **96**, 127403.
- H.-C. Weissker, H. B. Escobar, V. D. Thanthirige, K. Kwak, D. Lee, G. Ramakrishna, R. Whetten, and X. López-Lozano, *Nature Communications*, in press., 2014.
- P. Han and G. Bester, *Phys. Rev. B*, 2013, **88**, 165311.
- C. E. Patrick and F. Giustino, *Nat Commun*, 2013, **4**, 2006.
- R. Richter, D. Wolter, T. Zimmermann, L. Landt, A. Knecht, C. Heidrich, A. Merli, O. Dopfer, P. Reiss, A. Ehresmann, J. Petersen, J. E. Dahl, R. M. K. Carlson, C. Bostedt, T. Möller, R. Mitric and T. Rander, *Phys. Chem. Chem. Phys.*, 2014, **16**, 3070–3076.
- A. R. Van Sickle, J. B. Miller, C. Moore, R. J. Anthony, U. R. Kortshagen and E. K. Hobbie, *ACS Applied Materials & Interfaces*, 2013, **5**, 4233–4238.
- W. Yu, H. Feng, J. Wang, W. Dai, X. Yu, J. Zhang, W. Lai and G. Fu, *Physica B: Condensed Matter*, 2014, **434**, 177 – 180.
- V. Kocevski, O. Eriksson and J. Ruzs, *Phys. Rev. B*, 2013, **87**, 245401.
- C. Delerue, G. Allan and M. Lannoo, *Phys. Rev. B*, 1993, **48**, 11024.
- H.-Ch. Weissker, J. Furthmüller and F. Bechstedt, *Phys. Rev. B*, 2002, **65**, 155328.
- H.-Ch. Weissker, J. Furthmüller and F. Bechstedt, *Phys. Rev. B*, 2004, **69**, 115310.
- A. Tsolakidis and R. M. Martin, *Phys. Rev. B*, 2005, **71**, 125319.
- R. Guerra and S. Ossicini, *Phys. Rev. B*, 2010, **81**, 245307.
- A. N. Kholod, S. Ossicini, V. E. Borisenko and F. Arnaud d’Avitaya, *Phys. Rev. B*, 2002, **65**, 115315.
- D. V. Melnikov and J. R. Chelikowsky, *Solid State Communications*, 2003, **127**, 361.
- P. Logan and X. Peng, *Phys. Rev. B*, 2009, **80**, 115322.
- X. Sun, J. Liu, L. C. Kimerling and J. Michel, *Opt. Lett.*, 2009, **34**, 1198–1200.
- J. Liu, X. Sun, R. Camacho-Aguilera, L. C. Kimerling and J. Michel, *Opt. Lett.*, 2010, **35**, 679–681.
- L. B. Ma, T. Schmidt, O. Guillois and F. Huisken, *APL*, 2009, **95**, 013115.
- H.-Ch. Weissker, J. Furthmüller and F. Bechstedt, *Phys. Rev. Lett.*, 2003, **90**, 085501.
- S. Botti, H.-Ch. Weissker and M. A. L. Marques, *Phys. Rev. B*, 2009.
- S. Takeoka, M. Fujii, S. Hayashi and K. Yamamoto, *Phys. Rev. B*, 1998, **58**, 7921–7925.
- Y. Maeda, *Phys. Rev. B*, 1995, **51**, 1658.
- M. V. Wolkin, J. Jorne, P. M. Fauchet, G. Allan and C. Delerue, *Phys. Rev. Lett.*, 1999, **82**, 197.
- M. Luppi and S. Ossicini, *Phys. Rev. B*, 2005, **71**, 035340.
- L. E. Ramos, J. Furthmüller and F. Bechstedt, *Phys. Rev. B*, 2005, **72**, 045351.
- O. Sublemontier, F. Lacour, Y. Leconte, N. Herlin-Boime and C. Reynaud, *Journal of Alloys and Compounds*, 2009, **483**, 499.
- N. Chaâbane, V. Suendo, H. Vach and P. R. i Cabarrocas, *Applied Physics Letters*, 2006, **88**, 203111.
- H.-C. Weissker, N. Ning, F. Bechstedt and H. Vach, *Phys. Rev. B*, 2011, **83**, 125413.
- I. Vasiliev and R. M. Martin, *phys. stat. sol. (b)*, 2002, **233**, 5.
- A. Puzder, A. J. Williamson, F. A. Reboredo and G. Galli, *Phys. Rev. Lett.*, 2003, **91**, 157405.
- D. Dexter, in *Advances in Research and Applications*, ed. F. Seitz and D. Turnbull, Academic Press, 1958, vol. 6, pp. 353 – 411.
- H.-Ch. Weissker, J. Furthmüller and F. Bechstedt, *Phys. Rev. B*, 2003, **67**, 245304.
- M. Marsili, S. Botti, M. Palumbo, E. Degoli, O. Pulci, H.-C. Weissker, M. A. L. Marques, S. Ossicini and R. Del Sole, *The Journal of Physical Chemistry C*, 2013, **117**, 14229–14234.
- G. Kresse and J. Furthmüller, *Comput. Mat. Sci.*, 1996, **6**, 15.
- G. Kresse and D. Joubert, *Phys. Rev. B*, 1999, **59**, 1758.
- J. Jellinek and D. H. Li, *Phys. Rev. Lett.*, 1989, **62**, 241–244.
- M. E. Casida, *Recent Developments and Applications of Modern Density Functional Theory*, 1996, p. 391.
- M. A. L. Marques, A. Castro, G. F. Bertsch and A. Rubio, *Comp. Phys. Comm.*, 2003, **151**, 60.
- J. Derr, K. Dunn, D. Riabinina, F. Martin, M. Chaker and F. Rosei, *Physica E: Low-dimensional Systems and Nanostructures*, 2009, **41**, 668 – 670.
- A. Narayanaswamy, L. F. Feiner, A. Meijerink and P. J. van der Zaag, *ACS Nano*, 2009, **3**, 2539–2546.

-
- 51 P. Calcott, K. Nash, L. Canham, M. Kane and D. Brumhead, *Journal of Luminescence*, 1993, **57**, 257 – 269.
- 52 P. D. J. Calcott, K. J. Nash, L. T. Canham, M. J. Kane and D. Brumhead, *Journal of Physics: Condensed Matter*, 1993, **5**, L91.
- 53 C. Oghihara, Y. Inagaki, A. Taketa and K. Morigaki, *Journal of Non-Crystalline Solids*, 2012, **358**, 2004 – 2006.